UDC 519.65:519.68:624.07:691.3
Original scientific paper
Received: 30.12.2012.

Sensitivity analysis of numerical parameters in FEM/DEM model for RC structures

Nikolina Živaljić, Hrvoje Smoljanović and **Željana Nikolić**

University of Split, Faculty of Civil Engineering, Arhitecture and Geodesy, Matice Hrvatske 15, HR-21000 Split, CROATIA, e-mail: nikolina.zivaljic@gradst.hr

SUMMARY

The application of the finite-discrete element method (FEM/DEM) in the analysis of reinforced concrete (RC) structures is still in its early stages. Therefore, in this paper, sensitivity of the numerical model for analysis of RC structures based on the FEM/DEM method to the numerical parameters is presented. The accuracy of the solution, depending on the mesh refinement, crack spacing and penalty term, was analysed. The performed numerical analyses are useful in predicting the penalty parameter and mesh density in order to minimize numerical errors in analysis of RC structures with the FEM/DEM method. Validation of the numerical model for adopted numerical parameters was also shown by comparing numerical and experimental results.

Key words: *finite-discrete element method, reinforced concrete structures, mesh refinement, crack spacing, penalty term.*

1. INTRODUCTION

Most of the models for simulation of the behaviour of reinforced concrete (RC) structures, described in literature, are based on the finite element method (FEM), where the effect of cracking is modelled with the smeared or discrete crack approach. In the smeared crack approach [1-4], cracked concrete is represented as an elastic orthotropic material with reduced elastic modulus in the direction normal to the crack plane. With this continuum approach the local displacement discontinuities at cracks are distributed over some tributary area within the finite element, and the behaviour of cracked concrete can be represented by average stress-strain relations. In the discrete crack approach, cracks are formed as geometrical discontinuities by the separation of structural nodes [5] or by enriching the finite element shape function to enable capturing the discontinuity in the displacement field [6, 7]. However, the reported models are incapable of simulating the entire loading and failure process, particularly, the transition from continuum to discontinuum, and the interaction of the generated fragments that are typical of fracturing and fragmentation processes in reinforced concrete structures. Of late, the discrete element method based on modelling of the heterogeneous material by elementary particles held together by cohesive forces [8], which is firstly developed for granular soils, is extended to other heterogeneous brittle materials like concrete [9-11]. Recently, a discrete model based on Voronoi cell representation with the beam lattice network is used for modelling of brittle fracture phenomena for dynamic loading [12]. The damage phenomena in concrete can also be modelled with a continuum-discrete damage model [13, 14] which is capable of representing localized failure of massive structures. The improved deformability model within a discontinous deformation analysis was achieved either by introducing higher order strain fields by sub-block model [15].

Recently, the model for analysis and predicting the collapse of reinforced concrete structures based on the finite-discrete element method (FEM/DEM) was

developed [16]. This model is able to include effects of the behaviour of reinforced concrete structures under dynamic loading conditions in the linear-elastic stage, crack initiation and propagation, energy dissipation by non-linear effects, inertial effects due to motion, contact impact [17], and state of rest, which is a consequence of energy dissipation in the system [18].

Several numerical algorithms were developed and implemented in combined finite-discrete element code to realistically describe interactions between concrete and reinforcement, as well as general behaviour of RC structures. The model includes the cyclic behaviour of concrete and steel, an embedded model of reinforcing bars, the interaction between the reinforcement and concrete, the influence of adjacent cracks to the slip of reinforcing bar, local slip of reinforcing bar near the crack plane and the influence of the curvature of reinforcing bar to yield stress reduction of the steel. All developed algorithms are based on an approximation of the experimental curves for behaviour of the concrete and steel at a crack.

Numerical analyses of real RC structures based on the FEM/DEM method have shown that various parameters influence the accuracy of the results [16]. In this paper, the main characteristics of the developed numerical model were firstly presented. After that the influence of the numerical parameters to the accuracy of the solution was analyzed. At the end validation of the presented numerical model for a simply supported reinforced concrete beam exposed to monotonically increasing load up to failure is shown.

2. CONCRETE MATERIAL MODEL

Fracture and fragmentation processes are in essence processes of transition from continua to discontinua. In the FEM/DEM method, it is realized by a combined single and a smeared crack model.

In the model presented in this paper the behaviour of the concrete in compression is linear elastic while a stress–strain curve for concrete in tension is divided into two sections (Figure 1): strain-hardening prior to reaching the peak stress f_t, which is implemented through the constitutive law [19]; and strain-softening, which is based on an approximation of the experimental stress-displacement curves taken according to Hordijk [20].

The cracks are assumed to coincide with the finite element edges, which are achieved in advance through the topology of adjacent elements being described by different nodes. Separation of these edges induces a bonding stress which is taken to be a function of the size of separation δ (Figure 2). The area under stress-displacement curve represents the energy release rate $G_f = 2\gamma$, where γ is the surface energy, i.e. the energy needed to extend the crack surface by unit area.

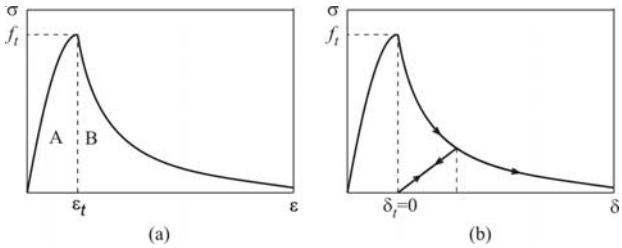

Fig. 1 (a) Strain hardening and strain softening curves defined in terms of strains; (b) Strain softening curve defined in terms of displacements

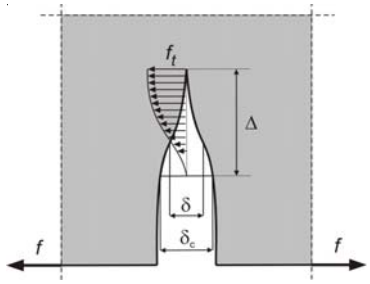

Fig. 2 Single crack model for the softening part of the stress-strain diagram

In theory the separation, $\delta = \delta_t = 0$ coincides with the bonding stress being equal to the tensile strength f_t, i.e., no separation occurs before the tensile strength is reached. In the actual implementation, it is enforced through the penalty function method [19].

For separation $\delta \le \delta_t$ the bonding stress is given by:

$$\sigma_c = \left[\frac{2\delta}{\delta_t} - \left(\frac{\delta}{\delta_t} \right)^2 \right] f_t \tag{1}$$

where $\delta_t = 2hf_t / p_0$ is the separation corresponding to the bonding stress being equal to the tensile strength f_t, h is the size of particular element and p_0 is penalty term at separation $\delta = 0$. In that way the separation of adjacent elements is normalized by the element size before reaching a tensile strength.

After reaching a tensile strength f_t stress decreases with an increasing separation δ and at $\delta = \delta_c$ bonding stress tends to zero. For separation $\delta_t < \delta < \delta_c$ bonding stress is given by:

$$\sigma_c = z f_t \tag{2}$$

where z is a heuristic scaling function representing an approximation of the experimental stress-displacement curves taken according to Hordijk [20]:

$$z = \left[1 + (c_1 D_t)^3 \right] e^{-c_2 D_t} - D_t (1 + c_1^3) e^{-c_2} \tag{3}$$

where $c_1 = 3$ and $c_2 = 6.93$, while the damage parameter D_t is determined according to following expression:

$$D_t = \begin{cases} (\delta - \delta_t)/(\delta_c - \delta_t), & if \quad \delta_t < \delta < \delta_c; \\ 1, & if \quad \delta > \delta_c \end{cases} \tag{4}$$

The edges of two adjacent elements are held together by shear stress calculated by using the penalty function method [21]. After reaching shear strength f_s, which coincides with sliding $t = t_s$, the stress

decreases with an increasing sliding t and at $t=t_c$ shear stress tends to zero. For sliding $t_s < |t| < t_c$ shear stress is given by:

$$\tau_c = (1 - D_s) f_s \tag{5}$$

where D_s is the damage parameter given by:

$$D_s = \begin{cases} (t - t_s)/(t_c - t_s), & if \quad t_s < t < t_c; \\ 1, & if \quad t > t_c \end{cases} \tag{6}$$

3. REINFORCEMENT MODEL

In this model the concrete structure was discretized with triangular finite elements, and the reinforcing bars were modelled with one-dimensional elements, which can be placed in arbitrary positions inside the concrete finite elements. The model of the reinforced concrete structure with an embedded reinforcing bar is shown in Figure 3.

The reinforcing bar was defined by its first and end points. Intersection between the sides of triangular concrete finite elements and reinforcing bars gives the reinforcement finite elements and reinforcement joint elements (Figure 3).

The structure behaves as a continuum until opening of the crack. In that phase the triangular concrete element and line element of the reinforcing bar behave as one body. The deformation of the triangular element influences the deformation of the reinforcing bar. It is assumed that the relationship between stress and strain in a finite element of the reinforcing bar is linear-elastic.

Appearance of a crack in the concrete, also leads to occurrence of a crack in the joint element in the concrete as well as a non-linear deformation in the joint element of a reinforcing bar.

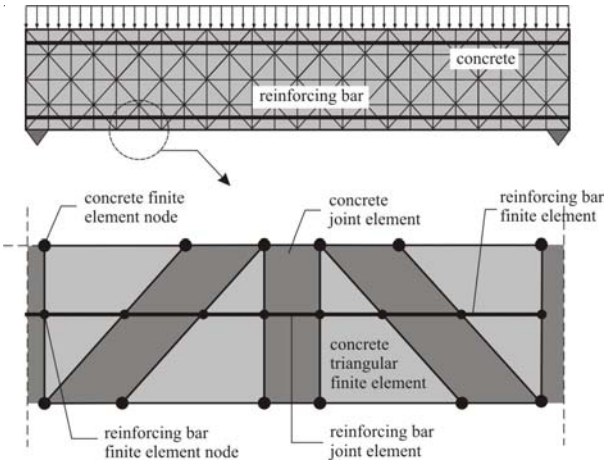

Fig. 3 Discretization of the reinforced concrete structure

The model of reinforcing bar in the joint element is divided into parts before and after the occurrence of a crack in the concrete. In theory, the separation $d = 0$ (Figure 4) coincides when the bonding stress is equal to the tensile strength of the concrete, i.e., no separation occurs before the tensile strength of concrete is reached. In this model, the continuity between the reinforcing bar finite elements is ensured through the penalty function method [21].

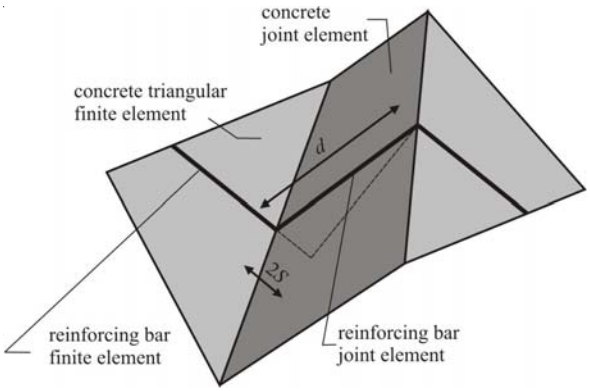

Fig. 4 Reinforcing bar joint element

After the occurrence of a crack in the concrete the numerical model of reinforcing bar joint element is based on a mechanical model for deformed reinforcing bars at reinforced concrete interface, developed by Soltani and Maekawa [22]. This model takes into account [16, 21]:

- the interaction between the reinforcement and concrete which was taken into consideration by steel strain-slip relation,
- local slip of reinforcing bar near the crack plane when the bar undergoes a high plastic deformation under reversed cyclic loading,
- the influence of the curvature of reinforcing bar to yield stress reduction of the steel,
- the cyclic behaviour of concrete and steel added to an existing combined single and smeared crack model, which is an essential mechanism for energy loss in the post-cracking response of the structure.

If the distance from an adjacent crack is small, the influence of adjacent cracks cannot be ignored. The influence of adjacent cracks is approximately taken into account through a reduction factor α [23], which depends on distance l_{cr} (Figure 5). The steel slip s_{cr}, which considers the influence of adjacent cracks, is expressed for monotonic loading as:

$$s_{cr} = \alpha s \tag{7}$$

where s is non-dimensional slip while reduction factor α is shown in Figure 5. Non-dimensional slip s is given by:

$$s = \left(\frac{S}{D}\right) K_{fc} \tag{8}$$

$$K_{fc} = \left(\frac{f_c}{20}\right)^{2/3} \tag{9}$$

where D is the diameter of the bar, f_c is the compressive strength of concrete (*MPa*) and S is slip shown in Figure 4.

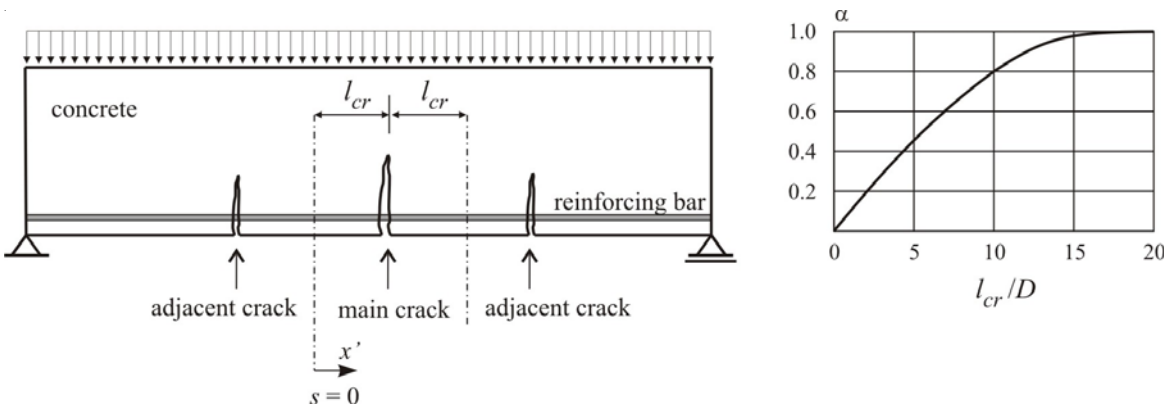

Fig. 5 Relation of reduction factor α and crack spacing l_{cr} in tension

4. ANALYSIS OF NUMERICAL PARAMETERS

In this section the influence of penalty parameter p_0, mesh refinement and crack spacing l_{cr} on the accuracy of the numerical results were analyzed.

4.1 Sensitivity of the model to the mesh refinement for tension

This example was chosen to analyze the sensitivity of the numerical model of the reinforcing bar to the mesh refinement and crack spacing l_{cr}. Analysis was performed on a reinforced concrete beam exposed to a monotonic increasing tension load as shown in Figure 6.

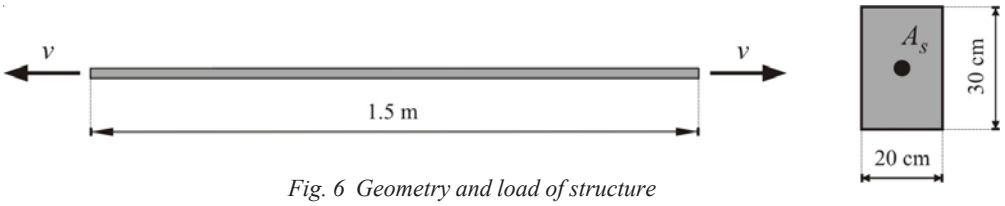

Fig. 6 Geometry and load of structure

Tension load was realized with constant velocity *v=0.1 m/s* in end points of beam. Material characteristics are shown in Table 1.

Table 1 Material characteristics of the beam

Concrete		***Steel***	
Modulus of elasticity , E_c (MPa)	*30 500*	*Modulus of elasticity , E_s (MPa)*	*190 000*
Poisson ratio , v	*0.2*	*Yield stress , f_y (MPa)*	*610*
Tensile strength , f_t (MPa)	*3.15*	*Ultimate stress , f_u (MPa)*	*750*
Compressive strength , f_c (MPa)	*40.0*	*Cross-section area , A_s (m^2)*	*0.0006*
		Bar diameter , D (m)	*0.008*

The beam was discretized with four different finite element meshes (A, B, C and D) shown in Figure 7. Mesh A is characterized by an element size of *h=15 cm*. Mesh B is comprised of finite elements of size *h=7.5 cm*, while meshes C and D are comprised of finite elements of size *h=5.0 cm*, and *h=3.75 cm* respectively.

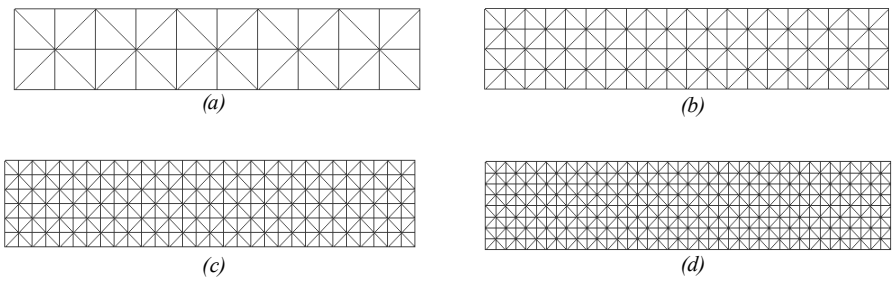

Fig. 7 Finite element meshes used in the analysis: (a) mesh A, (b) mesh B, (c) mesh C, (d) mesh D

Influence of adjacent cracks is considered with the parameter α which depends on crack spacing l_{cr}. In this example crack spacing is adopted as $l_{cr} = h / 2$.

Table 2 Value of parameter α for different mesh patterns

Mesh type / h	***Parameter α***
mesh A / h = 15 cm	*0.745*
mesh B / h = 7.5 cm	*0.406*
mesh C / h = 5.0 cm	*0.294*
mesh D / h = 3.75 cm	*0.242*

In Figure 8 relation between average stress defined as $\sigma = F / A$ and average deformation defined as $\varepsilon = \Delta l / l$ is shown.

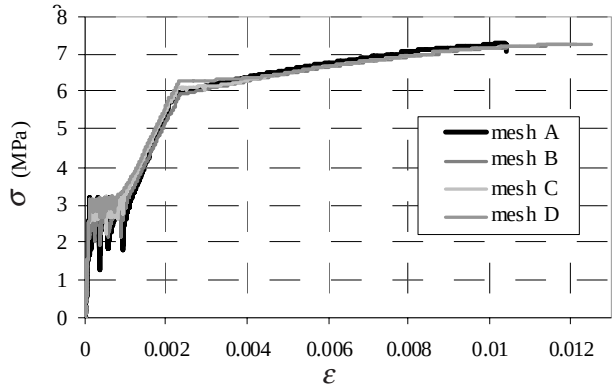

Fig. 8 The average stress – average strain relation for different mesh patterns

Failure patterns for different mesh type are shown in Figure 9.

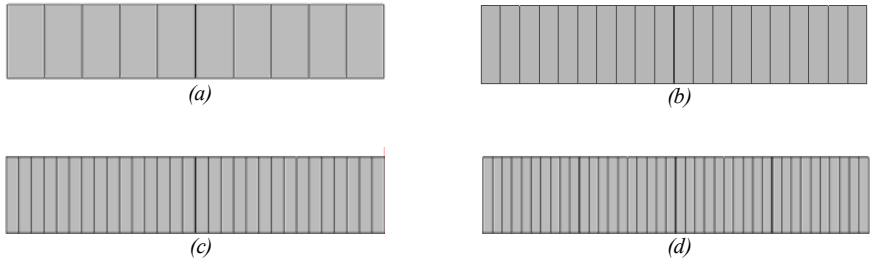

Fig. 9 Failure patterns for: (a) mesh A, (b) mesh B, (c) mesh C, (d) mesh D

The performed analysis indicates that the presented numerical model for reinforced bar is not significantly sensitive to mesh refinement or finite element size. Thus, the average stress and average strain relation in structure can be well described independent of crack spacing.

4.2. Sensitivity of the model to the penalty parameter for tension

This example was chosen to analyse the sensitivity of the numerical model of the reinforcing bar in the linear elastic stage to the penalty parameter p_0. Analysis was performed on a reinforced concrete cantilever exposed to a monotonic increasing tension load. Geometry and cross section of the structure are shown in Figure 10.

Material characteristics are shown in Table 3.

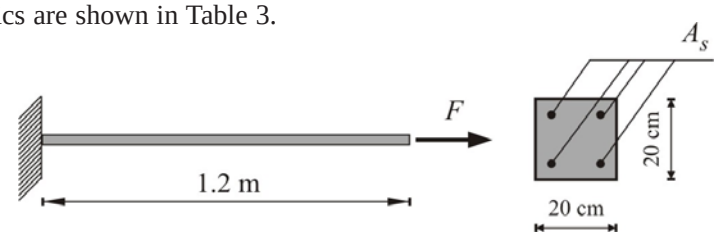

Fig. 10 Geometry and load of structure

Table 3 Material characteristics

Concrete		***Steel***	
Modulus of elasticity , E_c (MPa)	*30 500*	*Modulus of elasticity , E_s (MPa)*	*183 000*
Poisson ratio , v	*0.2*	*Yield stress , f_y (MPa)*	*420*
Tensile strength , f_t (MPa)	*3.15*	*Ultimate stress , f_u (MPa)*	*630*
		Cross-section area , A_s (m^2)	*0.00045*
		Bar diameter , D (m)	*0.012*

Discretization of structure is shown in Figure 11.

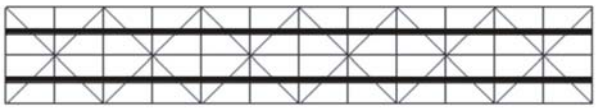

Fig. 11 Discretization of structure

Figure 12 shows the comparison of the analytical and numerical results obtained by the presented model for different penalty parameters.

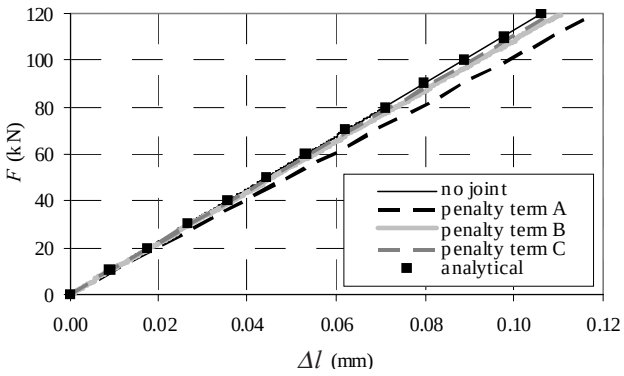

Fig. 12 Force-displacement relations

Relative errors in dependence on penalty parameters p_0 are shown in Table 4, where E_c is modulus of elasticity for concrete.

Table 4 Relative errors in dependence on penalty parameters

Penalty parameter		**Relative error (%)**
A	$20E_c$	*11.5*
B	$60E_c$	*3.50*
C	$100E_c$	*2.30*

The analysis shows that numerical results obtained without joint elements are identical to the analytical results. Numerical results obtained with joint elements have relative error which depends on the penalty parameter value. For higher penalty parameters, numerical results are closer to analytical results, but due to the numerical stability, it causes smaller time steps [24] and longer calculation time.

4.3. Sensitivity of the model to the mesh refinement for bending

This example was chosen to analyse the sensitivity of the finite-discrete element method to the mesh refinement in cases where influence of bending is dominant.

The analysis was performed on concrete cantilever subjected to monotonically increasing concentrated force at the end of the beam (Figure 13).

Material characteristics of the beam are shown in Table 5.

Table 5 Material characteristics of concrete

Concrete	
Modulus of elasticity , E_c (MPa)	*30 500*
Poisson ratio , v	*0.2*
Tensile strength , f_t (MPa)	*3.15*

The beam was discretized with three different finite element meshes (A, B and C) shown in Figure 14. Mesh A is characterized with four elements per beam high. Mesh B is comprised of six finite elements while mesh C comprised of eight finite elements per beam high.

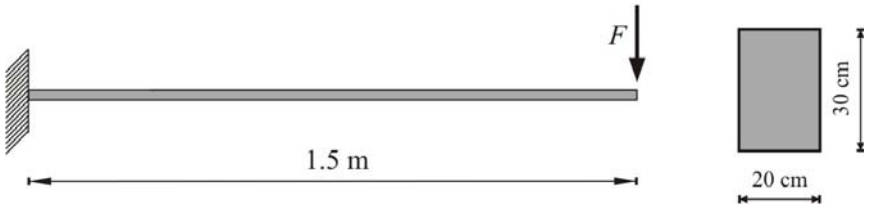

Fig. 13 Geometry and load of structure

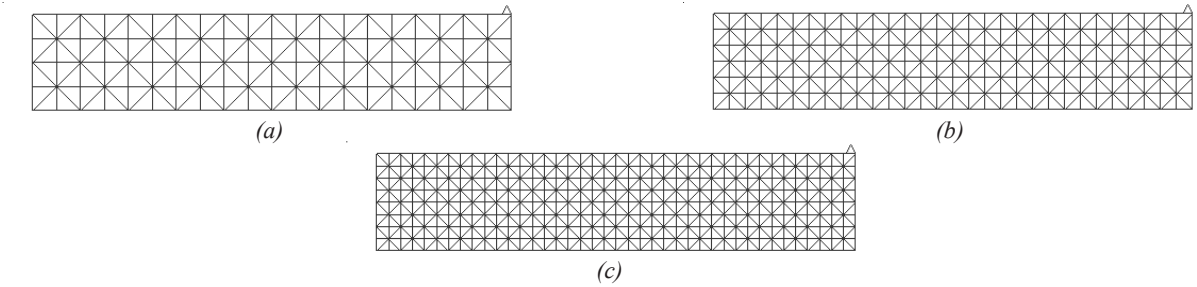

Fig. 14 Finite element meshes used in the analysis: (a) mesh A, (b) mesh B, (c) mesh C

Figure 15 shows comparison of the analytical and numerical (FEM/DEM) deflection of cantilever end for three different finite element mesh patterns.

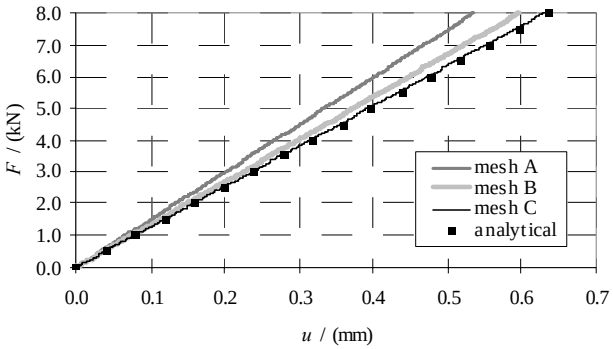

Fig. 15 Force-displacement relations for different mesh patterns

Relative errors in dependence on mesh patterns are shown in Table 6.

Table 6 Relative errors in dependence on mesh patterns

Mesh type	*Relative error (%)*
Mesh A 20E_c	*15.9*
Mesh B 60E_c	*7.40*
Mesh C 100E_c	*0.89*

The analysis shows that the minimum of eight finite elements per beam high are necessary to obtain an acceptable numerical error for cases where influence of bending is dominant. This finite element mesh pattern is adopted as basic in further analyses.

4.4. Sensitivity of the model to the penalty parameter for bending

This example was chosen to analyse the sensitivity of the numerical model of reinforcing bar to the penalty parameter p_0 for reinforced concrete structures where influence of bending is dominant. The cantilever reinforced concrete beam shown in Figure 16 was analysed. The beam was reinforced with two bars $2\phi 12$ *mm* in the upper zone and subjected to monotonically increasing concentrated force at the end of the beam.

Material characteristics and discretization of structure are shown in Table 7 and Figure 17, respectively.

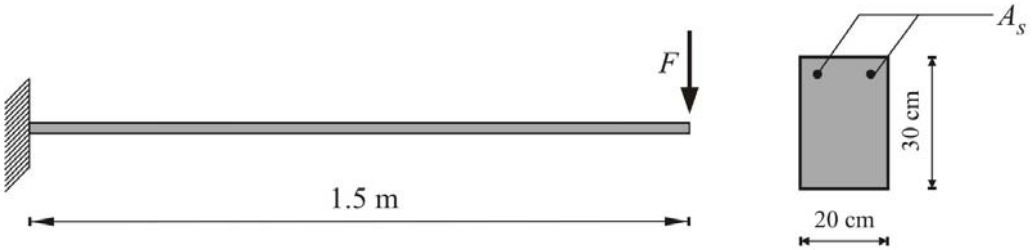

Fig. 16 Geometry and load of structure

Table 7 Material characteristics of the reinforced beam

Concrete		*Steel*	
Modulus of elasticity , E_c (MPa)	*30 500*	*Modulus of elasticity , E_s (MPa)*	*210 000*
Poisson ratio , ν	*0.2*	*Cross-section area , A_s (m^2)*	*0.00023*
Damping coefficient , ξ	0.0	*Bar diameter , D (m)*	*0.012*

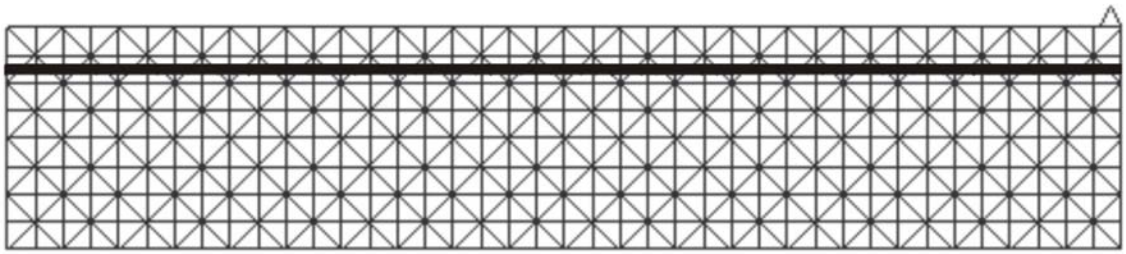

Fig. 17 Finite element mesh

Figure 18 shows the comparison of the numerical results obtained by programme ABAQUS [25] and numerical results obtained by using the presented model for different penalty parameters.

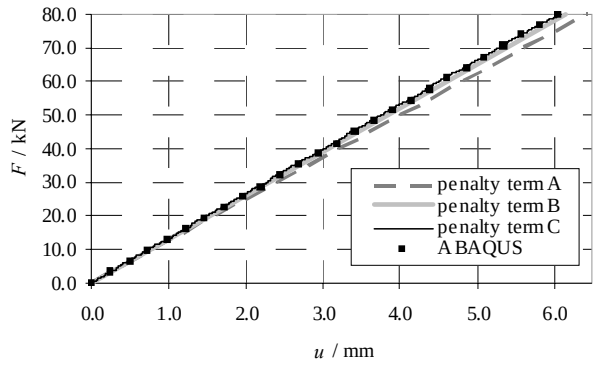

Fig. 18 Force-displacement relations

Relative errors in dependence on penalty parameters p_0 are shown in Table 8, where E_c is modulus of elasticity for concrete.

Table 8 Relative errors in dependence on penalty parameters

Penalty parameter		Relative error (%)
A	$20E_c$	6.42
B	$60E_c$	1.50
C	$100E_c$	0.65

The performed analysis shows that the error in the displacements is controlled through setting penalty p_0 as a function of the modulus of elasticity E_c. The analysis of influence of penalty to the error in displacement show that the relative error for $p_0 = 100\,E_c$ is less than *1%*. With the additional increasing of penalty, the displacement error is reduced.

In this example dynamic validation of presented model was performed with penalty parameter $p_0 = 100\,Ec$. After the force had reached the value of *80 kN*, it was momentarily removed and free oscillations of the beam appeared. The vertical displacement of the right-hand end of the cantilever beam was compared with the displacement obtained by the ABAQUS package (Figure 19) and shows excellent agreement of the results.

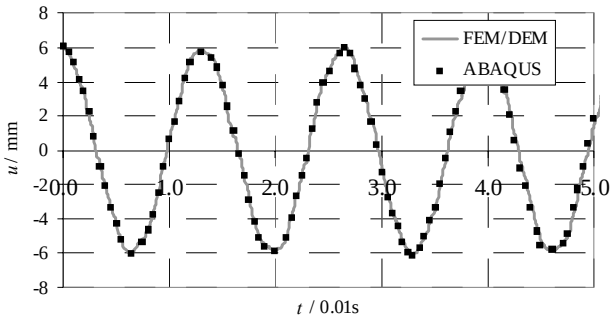

Fig. 19 Time-displacement curve at the end of the beam

5. VALIDATION OF THE MODEL

Validation of the presented numerical model is shown for a simply supported reinforced concrete beam exposed to a monotonically increasing load up to failure.

The characteristics of the beam are shown in Figure 20. This example was tested by Majewski and Krzowyon [26], both experimentally and numerically by the model based on the finite element method [27].

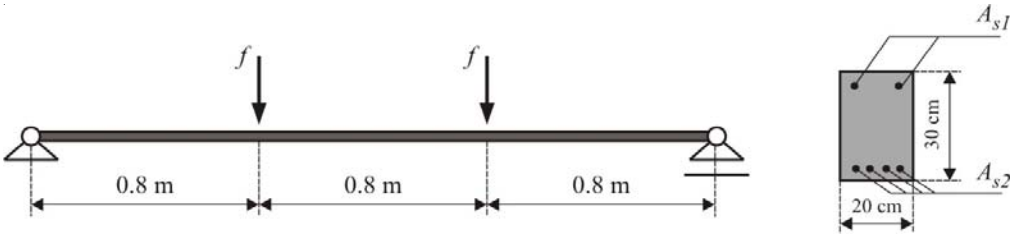

Fig. 20 Simply supported reinforced concrete beam

Material characteristics are taken from the literature and are shown in Table 9.

Table 9 Material characteristics of the beam

Concrete		Steel	
Modulus of elasticity, E_c / MPa	29 730	Modulus of elasticity, E_s / MPa	210 000
Poisson ratio, ν	0.2	Yield stress, f_y / MPa	420
Tensile strength, f_t / MPa	3.15	Cross-section area, A_{s1} / cm^2	1.02
Compressive strength, f_c / MPa	40.0	Cross-section area, A_{s2} / cm^2	4.52

The concrete structure was discretized into 1152 triangular elements while each reinforcing steel bar was modelled with 144 two-node elements. The load was increased until failure of the structure. The finite element mesh of the beam with reinforcement bars is shown in Figure 21.

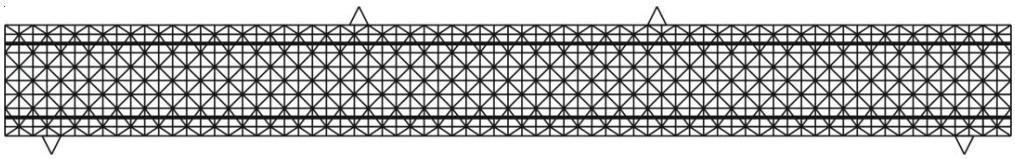

Fig. 21 Finite element mesh with reinforcement bars

Results of this model based on the FEM/DEM method were compared with the: (i) experimental results, (ii) numerical results obtained by the MAFEM programme for 2D non-linear finite element analysis [26], and (iii) numerical results obtained by the programme PRECON3D [27]. Comparisons of the displacements for the mid-span *d* of the beam until failure are shown in Figure 22.

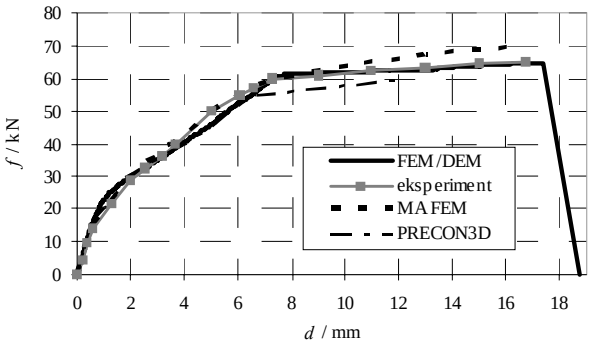

Fig. 22 Load-displacement curves for the mid-span of the beam

The load-displacement curve shows that the biggest deviation of the results obtained by FEM/DEM model in comparison with the experiment is *2.8%*. The failure load obtained by the code is *1.0%* lower than the experiment result. It can be noted that the FEM/DEM model gives better results with respect to the numerical results obtained by the MAFEM and the PRECON3D programmes which are based on non-linear finite element analysis.

The increase of stress in reinforcement steel which depends on the applied load is shown in Figure 23. The selected section is below the force *F* in the tensile reinforcing bar. The stress in reinforcement reached the yield stress at the moment of failure while the stress in the concrete was under the compressive strength of the concrete.

In this example, the failure of the structure occurs due to the yield of steel in tension which is an indication that the developed model for the reinforcement steel embedded in the FEM/DEM code is suitable for modelling the behaviour of RC structures until collapse.

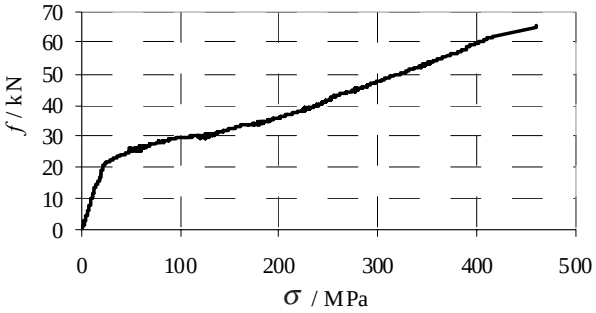

Fig. 23 Increase of stress in tensile reinforcing bar with applied load

The first crack that appeared for the force *f=56.6 kN*, is shown in Figure 24a. Cracks of the beam for different loads are shown in Figure 24.

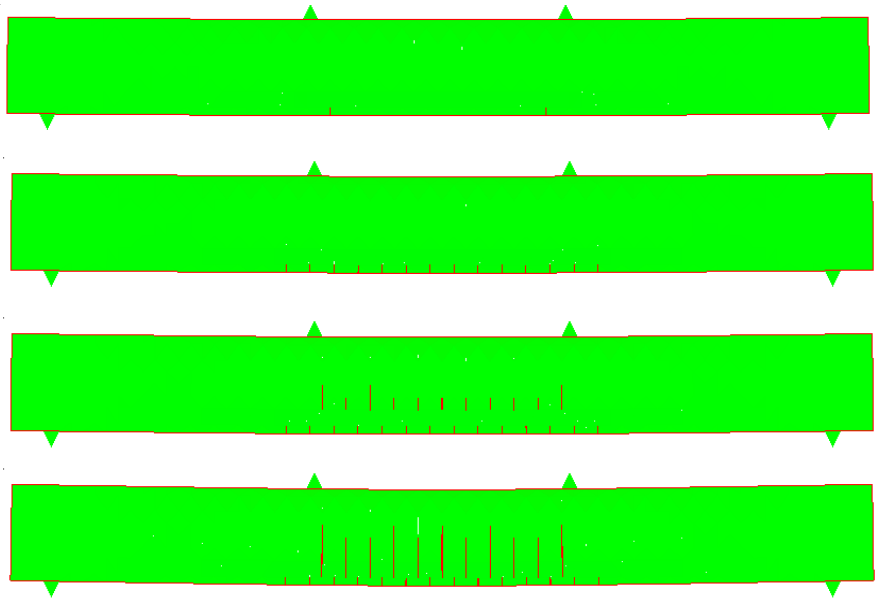

Fig. 24 The cracks of the beam for loads: (a) f=56.6 kN; (b) f=60.3 kN; (c) f=63.0 kN; (d)) f=64.0 kN

Figure 25 shows the beam at the moment of the collapse for the force *f=64.8 kN*.

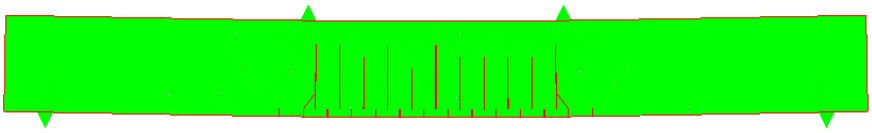

Fig. 25 The cracks of the beam at failure

5. CONCLUSION

The application of the finite-discrete element method (FEM/DEM) in the analysis of reinforced concrete structures is in its early stages. In this paper the influence of the numerical parameters to the accuracy of the solution obtained by presented model was analysed.

Numerical analyses performed in this paper are useful in predicting the penalty parameter and mesh density in order to obtain a reasonable numerical error in analysis of reinforced concrete structures with the FEM/DEM method.

The presented numerical example with adopted finite element mesh density and penalty term shows good agreement with experimental results and demonstrates the possibility of using the presented numerical model in the analysis of reinforced concrete structures.

6. ACKNOWLEDGEMENTS

The partial financial support, provided by the Ministry of Science, Education and Sports of the Republic of Croatia under the project *Non-linear Dynamic Analysis of Three-dimensional Reinforced Concrete Structures*, is gratefully acknowledged.

7. REFERENCES

[1] Y.R. Rashid, Analysis of prestressed concrete pressure vessels, *Nuclear Engineering and Design*, Vol. 7, No 4, pp. 334-344, 1968.

[2] Z.P. Bažant and L. Cedolin, Fracture mechanics of reinforced concrete, *ASCE Journal of the Engineering Mechanics*, Vol. 106, No. 6, pp. 1287-1306, 1980.

[3] V. Travaš, J. Ožbolt and I. Kožar, Failure of plain concrete beam at impact load: 3D finite element analysis, *Int. J. of Fracture*, Vol. 160, No. 1, pp. 31-41, 2009.

[4] J. Ožbolt, D. Meštrović and I. Kožar, Three-dimensional analysis of overreinforced concrete girders, *Građevinar*, Vol. 58, No. 2, pp. 95-101, 2006. (in Croatian)

[5] D. Ngo and A.C. Scordelis, Finite element analysis of reinforced concrete beams, *Journal of ACI*, Vol. 64, No. 3, pp. 152-163, 1967.

[6] T. Belytschko and T. Black, Elastic crack growth in finite elements with minimal remeshing, *Int. J. for Numerical Methods in Engineering*, Vol. 45, pp. 601–620, 1999.

[7] N. Moës, J. Dolbow and T. Belytschko, CA finite element method for crack growth without remeshing, *Int. J. for Numerical Methods in Engineering*, Vol. 46, pp. 131–150, 1999.

[8] P.A. Cundall and A.D.L. Strack, A discrete numerical model for granular assemblies, *Geotechnique*, Vol. 29, No. 1, pp.47-65, 1979.

[9] E. Schlangen and E.J. Garboczi, Fracture simulation of concrete using lattice models: Computational aspects, *Engineering Fracture Mechanics*, Vol. 57, No. 2/3, pp. 319–332, 1997.

[10] G.A. D'Addetta, E. Kuhl, F. Kun and E. Ramm, Micromechanical modeling of concrete cracking, Proc. of European Conference on Computational Mechanics, ECCM'99. Munich, Germany, 1999.

[11] M. Ortiz and A. Pandolfi, Finite-deformation irreversible cohesive elements for three-dimensional crack-propagation analysis, *Int. J. for Numerical Methods in Engineering*, Vol. 44, pp. 1267–1282, 1999.

[12] A. Ibrahimbegović and A. Delaplace, Microscale and mesoscale discrete models for dynamic fracture of structures built of brittle materials, *Computers and Structures*, Vol. 81, 1255-1265, 2003.

[13] D. Brancherie and A. Ibrahimbegović, Novel anisotropic continuum-discrete damage model capable of representing localized failure of massive structures, Part I: Theoretical formulation and numerical implementation, *Engineering Computations*, Vol. 26, No. 1/2, pp. 100-127, 2009.

[14] A. Kucerova, D. Brancherie, A. Ibrahimbegović, J. Zeman and Z. Bittnar, Novel anisotropic continuum-discrete damage model capable of representing localized failure of massive structures, Part II: Identification from tests under heterogeneous stress field, *Engineering Computations*, Vol. 26, No. 1/2, pp. 128-144, 2009.

[15] C.J. Pearce, A. Thavalingam, Z. Liao and N. Bićanić, Computational aspects of the discontinuous deformation analysis framework for modelling concrete fracture, *Engineering Fracture Mechanics*, Vol 65, pp. 283-298, 2000.

[16] N. Živaljić, Finite-discrete element method for 2D seismic analysis of RC structures, Ph.D. Thesis, University of Split, Faculty of Civil Engineering, Architecture and Geodesy, Split, 2012. (in Croatian)
[17] A. Munjiza, K.R.F. Andrews and J.K. White, Penalty function method for combined finite-discrete element system comprising large number of separate bodies, *Int. J. for Numerical Methods in Engineering*, Vol. 49, pp. 1377-1396, 2000.
[18] T. Bangash and A. Munjiza, Experimental validation of a computationally efficient beam element for combined finite-discrete element modelling of structures in distress, *Computational Mechanics*, Vol. 30, pp. 366-373, 2003.
[19] A. Munjiza, K.R.F. Andrews and J.K. White, Combined single and smeared crack model in combined finite-discrete element method, *Int. J. for Numerical Methods in Engineering*, Vol. 44, pp. 41-57, 1999.
[20] D.A. Hordijk, Tensile and tensile fatigue behaviour of concrete – experiments, modelling and analyses, *Heron*, Vol. 37, No. 1, pp. 3-79, 1992.
[21] N. Živaljić, H. Smoljanović and Ž. Nikolić, A combined finite-discrete element model for RC structures under dynamic loading, *Engineering Computations,* 2013. (accepted for publication)
[22] M. Soltani and K. Maekawa, Path-dependent mechanical model for deformed reinforcing bars at RC interface under coupled cyclic shear and pullout tension, *Engineering Structures*, Vol. 30, pp. 1079-1091, 2008.
[23] K. Maekawa, A. Pimanmas and H. Okamura, *Nonlinear Mechanics of Reinforced Concrete*, Spon Press, London, 2003.
[24] A. Munjiza and N.W.M. John, Mesh size sensitivity of the combined FEM/DEM fracture and fragmentation algorithms, *Engineering Fracture Mechanics*, Vol. 69, pp. 281-295, 2002.
[25] ABAQUS Version 6.10 Documentation, Dassault Systémes Simulia Corporation, 2010.
[26] S. Majewski and R. Krzywon, Numerical and experimental verification of FEM for elastoplastic analysis of RC structures and soil structure interaction problems, Proc. of the 7th Int. Conf. on Numerical Methods in Continuum Mechanics, High Tatras, October 1998, Eds. V. Kompiš, M. Žmindak and B. Hučko, University of Žilina, Žilina, pp. 519-524, 1998.
[27] M. Galić, P. Marović and Ž. Nikolić, Modified Mohr-Coulomb - Rankine material model for concrete, *Engineering Computations*, Vol. 28, No. 7, pp. 853-887, 2011.

ANALIZA UTJECAJA NUMERIČKIH PARAMETARA U FEM/DEM MODELU ZA AB KONSTRUKCIJE

SAŽETAK

Primjena metode konačno-diskretnih elemenata (FEM/DEM) u analizi armirano-betonskih konstrukcija je u samom začetku. Stoga je u ovom radu analiziran utjecaj numeričkih parametara na osjetljivost numeričkog modela za analizu AB konstrukcija zasnovanog na FEM/DEM metodi. Analiziran je utjecaj gustoće mreže, udaljenosti pukotina i penalty parametra na točnost rješenja. Provedene numeričke analize omogućuju pravilan odabir penalty parametra i gustoće mreže s ciljem minimiziranja numeričke pogreške u analizi AB konstrukcija FEM/DEM metodom. Validacija numeričkog modela za usvojene numeričke parametre također je pokazana usporedbom numeričkih i eksperimentalnih rezultata.

***Ključne riječi**: metoda konačno-diskretnih elemenata, armirano-betonske konstrukcije, gustoća mreže, udaljenost pukotina, penalty parametar.*